A 30-month Field Evaluation of Low-Cost CO_2 Sensors Using a Reference Instrument

Qixiang Cai[1,2], Ning Zeng[3*], Xiaoyu Yang[4], Chi Xu[5], Zhaojun Wang[4], Pengfei Han[6,7*]

[1]State Key Laboratory of Numerical Modeling for Atmospheric Sciences and Geophysical Fluid Dynamics, Institute of Atmospheric Physics, Chinese Academy of Sciences, Beijing 100029, China

[2]Qiluzhongke Institute of Carbon Neutrality, Jinan 250100, China

[3]Department of Atmospheric and Oceanic Science, and Earth System Science Interdisciplinary Center, University of Maryland, College Park, Maryland 20742, USA

[4]Shandong Jinan Ecological and Environmental Monitoring Center, Jinan 250102, China

[5]State Environmental Protection Key Laboratory of Quality Control in Environmental Monitoring, China National Environmental Monitoring Centre, Bejing 100012, China

[6]State Key Laboratory of Atmospheric Environment and Extreme Meteorology, Institute of Atmospheric Physics, Chinese Academy of Sciences, Beijing 100029, China

[7]Carbon Neutrality Research Center, Institute of Atmospheric Physics, Chinese Academy of Sciences, Beijing 100029, China

Correspondence to: Pengfei Han (pfhan@mail.iap.ac.cn); Ning Zeng (zeng@umd.edu)

Abstract. CO_2 monitoring networks with low-cost and medium-precision sensors (LCSs) have become an exploratory direction for CO_2 observation under complex emission conditions in cities. Yet the performance of such LCS after deployment in the field faces significant challenges due to environmental impacts (e.g., temperature and humidity) and long-term drifts due to sensor degradation (e.g., the light source). Here, we conducted 30 months of co-located observations using LCS instruments (named SENSE-IAP) with a reference instrument (Picarro) to study the long-term performance of the LCSs under field conditions, which is essential for the correction and validation of mid-low cost CO_2 observation networks. The environmental correction system we developed effectively corrected the impact of daily environmental changes, which reduced the root mean square errors (RMSE) from 5.9 ± 1.2 ppm to 1.6 ± 0.5 ppm for SENSE-IAP. The corrections remained robust against seasonal environmental variations, and the daily RMSE was generally 1-3 ppm over the 30 months of observation. Long-term drifts, commonly occurring in LCS, resulted in biases reaching up to 27.9 ppm over two years. Furthermore, the seasonal drift cycle contributed an RMSE of up to 25 ppm after six months of the deployment. While the environmental correction system could not correct these errors, a linear interpolation method effectively corrected the long-term drift. The long-term drift correction significantly decreased the RMSE to 2.4 ± 0.2 ppm over the 30-month observation. To improve the accuracy of high-density CO_2 networks utilizing LCSs, we recommend that the calibration frequency is better within three months and not exceed six months, with optimal calibration performed during winter and summer to maintain daily accuracy within 5 ppm. These findings suggest that SENSE-IAP instruments can be

deployed for a long period without the need for taking back to re-calibrate in the laboratory or frequent standard gas calibration in the field, thereby significantly reducing time, labor, and financial costs.

Keywords: low-cost sensors; environmental correction; long-term drift calibration; CO_2 monitoring network

1. Introduction

Urban CO_2 emissions demonstrate complex spatial and temporal variability (Wada et al., 2011), influenced by diverse emission sources (Gurney et al., 2012; Kellett et al., 2013), meteorological factors (Grimmond et al., 2002; Lateb et al., 2016) and potential misinterpretation from biogenic fluxes (Miles et al., 2021). These complexities pose significant challenges in accurately capturing and interpreting the intricate changes in urban CO_2 concentrations, highlighting the necessity for more advanced and comprehensive monitoring solutions.

Recent advancements in medium-precision carbon monitoring technologies have made establishing high-density, low- and mid-cost, and medium-precision sensor networks a viable and competitive strategy (Müller et al., 2020; Shusterman et al., 2018). This approach effectively addresses the challenges associated with the variability of CO_2 in urban environments, which are characterized by complex emission sources, vegetation carbon sinks, and dynamic meteorological conditions. In contrast to high-precision (0.1 ppm) instruments like Picarro cavity ring-down spectroscopy (CRDS) analyzer (Picarro, 2023) at prices of ~ 100 000 USD, low- ($30 - $500) and mid-cost ($1,000 - $5,000) sensors using non-dispersive infrared detection (NDIR) (Table 1) (Han et al., 2025) offer an accuracy range of 1-10 ppm and are more cost-effective, with prices reduced by more than an order of magnitude (30-5000 USD). This cost efficiency enables large-scale deployment, making low- and mid-cost sensors an attractive option for comprehensive urban CO_2 monitoring (Lopez-Coto et al., 2017; Turner et al., 2016; Wu et al., 2016; Zeng et al., 2021).

Table 1. Types of low-cost and mid-cost sensors.

Sensor type	Typical cost range (US$)	Typical precision (ppm CO_2)	CO_2 sensors	Network
Low-cost	$30 - $500	1-10 ppm	SenseAir LP8; SenseAir K30	Switzerland, Carbosense CO_2 sensor network (Müller et al., 2020) Beijing, SENSE-JJJ (Han et al., 2024)
Mid-cost	$1,000 - $5,000	1 - 4 ppm	Vaisala GMP343; SenseAir HPP	California, BEACO$_2$N (Asimow et al., 2024) Switzerland, ZiCOS-M (Grange et al., 2025) Paris, CO_2 sensor Network (Lian et al., 2024)

While cost-effective, NDIR sensors are sensitive to environmental changes and often exhibit long-term drifts and abrupt jumps. Noise, environmental sensitivity, and temporal drifts result in raw measurements that typically have more

删除[其骧 才]: cost
删除[其骧 才]: (LCS)
删除[其骧 才]: (Picarro, 2020) or ABB-LGR
删除[其骧 才]: LCSs
删除[其骧 才]: 1
删除[其骧 才]: 10
删除[其骧 才]: 5-15 thousand
删除[其骧 才]:
删除[其骧 才]: LCS
删除[韩鹏飞 [2]]: **C**
删除[韩鹏飞 [2]]: –
删除[其骧 才]: low-cost non-dispersive infrared (
删除[其骧 才]:) sensors,
删除[其骧 才]: from LCS

significant errors and uncertainties than the accuracy and resolution required for urban CO_2 monitoring. The accuracy of such sensors generally depends on the correction methods that account for factors such as temperature, humidity, and pressure. The sensitivities of these instruments to environmental variables are inconsistent, posing significant challenges in calibrating many sensors (Bigi et al., 2018; Delaria et al., 2021; Hagan et al., 2018; Martin et al., 2017). Through careful correction using environmental chambers and collocated high-precision instruments these sensors can achieve short-term measurement accuracy within ± 1-3 ppm under laboratory conditions (Cai et al., 2024; Grange et al., 2024; Müller et al., 2020).

Additionally, compared to the stability of high-precision instruments, NDIR sensors are more susceptible to temporal drift and fluctuations. To address the above issues, sensors are taken to the laboratory for regular correction or undergo in-situ field calibration using traceable standard gases. These correction processes, while essential, are labor-intensive and require substantial time investment. Some networks employ alternative approaches. For instance, sensor-specific drift slope can be determined before deployment, and the offset can be corrected by the lower percentile of observations (5-10%) of the entire network (Shusterman et al., 2016). Delaria et al. (2021) proposed that by using the median value from at least 12 sites with small temperature dependence as a reference, the network precision can be maintained at 3.6 ppm. Another approach is that, the drift can be determined through nearby instruments under specific weather conditions during which horizontal gradients in CO_2 are small (Müller et al., 2020). One robust and commonly used calibration method is automatic/manual standard gas. We used this standard gas method in the Beijing and Jinan networks with more than 160 instruments, the calibration frequency is one week for automatic standard gas, and the results showed mean biases -1.28 ~ -0.64 ppm with standard gas at one month scale (Cai et al., 2024). The manual standard gas calibration is useful in mobile observations such as on-road observations using vehicles and vertical profile observations using tethered balloons (Liu et al., 2021; Bao et al., 2020). The calibration cost using automatic standard gas (1 week frequency) can reach $300/station/year, which consumes 2 tanks of 8L 10 MPa gas (one tank work standard gas, and one tank target/quality-check standard gas). And thus 100 stations using such LCS sensors will cost $30,000/year for standard gas.

Currently, several cities such as California, Paris, Switzerland and Beijing have established high-density CO_2 monitoring networks utilizing NDIR sensors (Table 1). For instance, the Berkeley Environmental Air-quality and CO_2 Network (BEACO$_2$N) in California, USA, utilizes the Vaisala CarboCap GMP343 sensor (mid-cost), with a raw accuracy of ± 3ppm+1% reading (Vaisala, 2020). After correcting for bias and temporal drift using the in-situ method, the observation accuracy is approximately 1-4 ppm (Shusterman et al., 2016, 2018), while the reported accuracy improved to 1.6-3.6 ppm after temperature correction (Delaria et al., 2021). The Carbosense CO_2 sensor network in Switzerland (Müller et al., 2020), which uses the SenseAir LP8 sensor (low-cost), with a raw accuracy of ± 50 ppm (SenseAir: LP8 Product Sheet, 2019),

删除[其骧 才]: Consequently, the accuracy of such sens

删除[韩鹏飞]:

删除[其骧 才]: requently against a mobile standard

删除[其骧 才]: ultiple

设置格式[其骧 才]: 字体: （默认）Times New Roman

删除[其骧 才]: successfully

删除[其骧 才]: 2this type of temperature dependence and

删除[其骧 才]:

删除[其骧 才]: an alternative method

设置格式[韩鹏飞]: 字体: （中文）宋体, 10 磅, 字体

设置格式[韩鹏飞]: 字体: （中文）宋体, 10 磅, 字体

设置格式[韩鹏飞]: 字体: （中文）宋体, 10 磅, 字体

设置格式[韩鹏飞]: 字体: （中文）宋体, 10 磅, 字体

设置格式[韩鹏飞]: 字体: （中文）宋体, 10 磅, 字体

设置格式[韩鹏飞]: 字体: （中文）宋体, 10 磅, 字体

删除[韩鹏飞 [2]]: 2000 RMB yuan

设置格式[韩鹏飞]: 字体: （中文）宋体, 10 磅, 字体

设置格式[韩鹏飞]: 字体: （中文）宋体, 10 磅, 字体

设置格式[韩鹏飞]: 字体: （中文）宋体, 10 磅, 字体

设置格式[韩鹏飞]: 字体: （中文）宋体, 10 磅, 字体

设置格式[韩鹏飞]: 字体: （中文）宋体, 10 磅, 字体

设置格式[韩鹏飞]: 字体: （中文）宋体, 10 磅, 字体

删除[韩鹏飞 [2]]: 0.2

设置格式[韩鹏飞]: 字体: （中文）宋体, 10 磅, 字体

删除[韩鹏飞 [2]]: million RMB yuan

设置格式[韩鹏飞]: 字体: （中文）宋体, 10 磅, 字体

设置格式[韩鹏飞]: 字体: （中文）宋体, 10 磅, 字体

设置格式[韩鹏飞]: 字体: （中文）宋体, 10 磅, 字体

删除[其骧 才]: of obtaining a reference for the determin

设置格式[其骧 才]: 字体: （默认）Times New Roman,

achieves an observation accuracy of 8-12 ppm through initial laboratory chamber correction and regular drift calibration via ambient co-location with nearby reference instruments.

China aims at peaking carbon emissions before 2030 and achieving carbon neutrality before 2060 (the Dual Carbon Goals, DCGs) (He et al., 2020; Huang et al., 2023; Zeng et al., 2022). To support China's DCGs and address the high spatial variability of CO_2 concentration in urban areas, the Institute of Atmospheric Physics, Chinese Academy of Sciences (IAP), established a network of 134 sites using SenseAir K30 sensor since 2017 (Han et al., 2024). This study presents the correction methods developed for the SenseAir K30 sensors and evaluates the accuracy achievable through the environmental dependence correction method based on laboratory simulation. At a field observation site in Beijing, environmentally corrected low-cost sensors (LCSs) were co-located with high-precision Picarro instruments for up to 30 months. By comparing the data with measurements from Picarro instruments, we gained more profound insights into the long-term performance and long-term drift characteristics of the LCS, as well as assessed the effectiveness of our long-term drift correction method. Our findings demonstrate that timely long-term drift correction significantly improved the accuracy of urban CO_2 monitoring networks based on LCS and reduced time, labor, and money investment. This research provides valuable evidence for optimizing the deployment and maintenance of LCS-based monitoring networks in urban environments.

删除[其骧 才]: To address the above issues, sensors are taken to the laboratory for regular correction or undergo in situ field calibration using traceable standard gases. These correction processes, while essential, are labor-intensive and require substantial time investment.

删除[韩鹏飞]: ed

删除[其骧 才]: dual carbon goal

删除[韩鹏飞]: deployed to

删除[其骧 才]: -

2. The application of SenseAir K30 sensors for urban CO_2 monitoring

A multivariate linear regression analysis was used for environmental correction, which can improve the accuracy of the SenseAir K30 sensor from its initial specification of ± 30 ppm ± 3 % of reading (SenseAir: K30 products sheets, 2022) to a range of 1.7-4.3 ppm (Martin et al., 2017). The environmentally corrected K30 sensor demonstrated reliability and consistency when compared to higher-precision instruments and standard gas under a controlled indoor environment, with a root mean square error (RMSE) ranging from 1 to 3 ppm on a monthly scale (Cai et al., 2024). Furthermore, the low-cost sensor exhibited highly consistent with Picarro system during on-road observations conducted using the same vehicle, with an RMSE of 3.6 ppm (Liu et al., 2021). In a study by Bao et al., (2020), the sensor was utilized to measure the CO_2 vertical profile in the lower troposphere in Hebei Province, China, showing good consistency with traditional gas chromatography measurements (Bao et al., 2020). Additionally, Cai et al., (2024) applied the low-cost sensor in an industrial park, revealing a CO_2 concentration enhancement of 5-28 ppm within the park compared to a reference site (Cai et al., 2025).

The Beijing-Tianjin-Hebei (or Jing-Jin-Ji, JJJ) network, deployed with low-cost sensors, has provided valuable insights into seasonal variations, urban-rural differences, and the homology of CO_2 and $PM_{2.5}$ (Han et al., 2024). The low-cost

删除[其骧 才]: quality

删除[韩鹏飞]: (

sensors have also been proven effective in detecting signals related to COVID-19. Continued CO_2 measurements in Beijing showed a 15-ppm reduction during the 2020 lockdown period compared to the before and after periods. Similarly, regular on-road CO_2 observation in Beijing before, during, and after COVID-19 lockdown showed a 40–60ppm decrease during COVID-19 lockdown period (Liu et al., 2021). These applications demonstrate the versatility and reliability of low-cost sensors in capturing both environmental and anthropogenic influences on atmospheric CO_2 concentrations.

3. Instrument design and correction methods of SENSE-IAP

The SENSE-IAP instrument integrates three K30 sensors alongside a Bosch BME680 (BME) sensor (Bao et al., 2020; Liu et al., 2021) , all collected by an updated version of BeagleBone Green Wireless (BBGW). The standard version of SENSE-IAP instrument also includes a Figaro TGS 2611 sensor for CH_4 detection and a Plantower PMSA003 for $PM_{2.5}$ measurements. These components are compactly integrated onto a single circuit board and housed within a weatherproof enclosure, as illustrated in Fig. 1.

The BME sensor is positioned close to the K30s to simultaneously monitor the temperature (T in ℃), relative humidity (RH in %), and pressure (P in hpa) of the air mass inside the instrument. This design ensures real-time correction of the sensor response values, accounting for dynamically changing external environmental conditions and enhancing measurement accuracy.

Figure 1. The layout of sensors in the standard version of SENSE-IAP instrument.

To improve the observing accuracy, we developed a CO_2 calibration system including both controlled environmental experiments and calibration software (Bao et al., 2020; Han et al., 2024; Liu et al., 2021), which has the main following steps:

设置格式[韩鹏飞]: 下标

1) raw electrical signals were converted to CO_2 values around atmospheric observation ranges; 2) data were then resampled from 2s to 1 minute to reduce white noise; 3) environmental corrections of temperature, humidity and air pressure for span calibration; 4) calibration by standard gas traceable to the WMO X2007 scale, similar to the standard used at high precision systems (such as Picarro instruments), to remove system bias. It was generally one week period of co-location with reference instrument for controlled environmental experiments to determine the environmental correction coefficients of the sensors, and another week co-location for post-quality check. And to fully understand the characteristics of long-term drift, at least one year is recommended to include the seasonal cycle (both summer and winter).

The raw signals from all sensors were collected at a frequency of 2 seconds, with a standard deviation of approximately ± 4 ppm. Fig. 2 shows the experimental results of continuously introducing standard gas over 25 hours to evaluate the instrument's noise characteristics. As shown in Fig. 2, the Allan deviation (in ppm) decreases with increasing integration time. At a 2-second measurement interval, the noise level is 4 ppm, which decreases to approximately 0.2 ppm for integration times ranging from 2 minutes to 1 hour. However, the Allan deviation increases after 1 hour of integration time, indicating the presence of drift contributions.

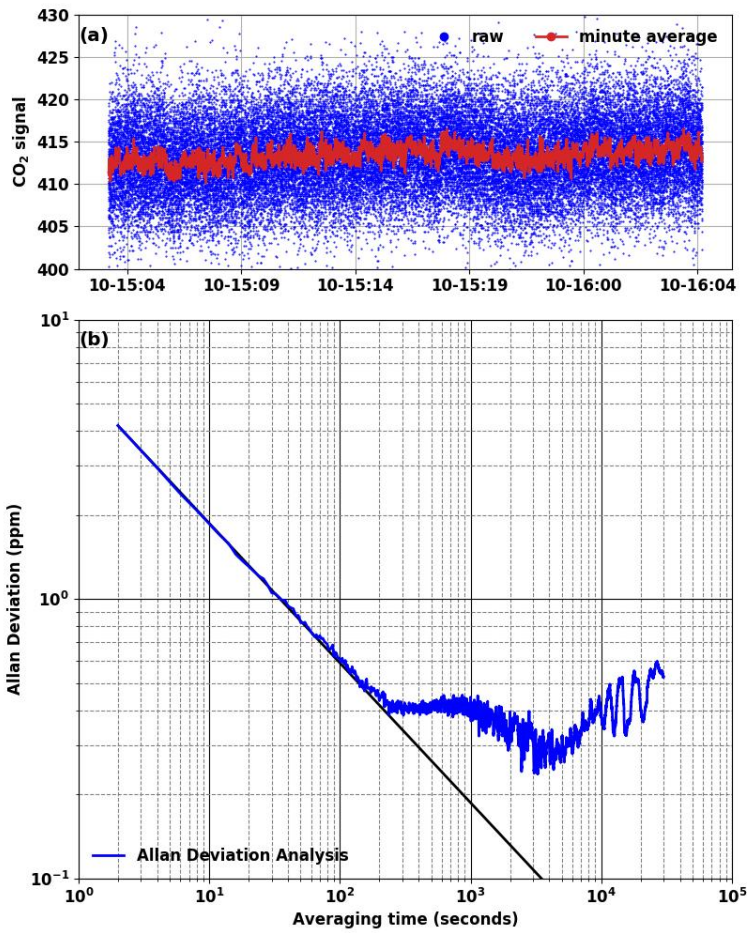

Figure 2. (a) The raw signals measured continuously over 25 hours from 03:00 on October 15th to 03:00 on October 16th, 2022. (b) Allan deviation log plots.

设置格式[韩鹏飞]: 字体: 10 磅, 字体颜色: 黑色

设置格式[韩鹏飞]: 字体: （中文）宋体, 10 磅, 字体颜色: 黑色

删除[其骧 才]: background noise

删除[其骧 才]: level

删除[其骧 才]: 20

In addition to white noise, the raw signals often contain outliers that must be removed through quality control. According to formula 1, following the 3-sigma principle, the original data points xi collected during the sampling period are treated as samples. The average value $\bar{x}$ of non-missing x_i is calculated, along with the standard deviation (SD) of the xi is σ. If |xi-$\bar{x}$|>4 σ, the data point is identified as an outlier and removed. We adopted the 4σ threshold to strike a balance between effectively removing outliers and preserving the natural ranges of variability in the data.

$$\sigma = \sqrt{\frac{\sum_{i=1}^{n}(x_i-\bar{x})^2}{n-1}} \quad (1)$$

Subsequently, the raw signals are averaged from a 2-second interval to a 1-minute interval (resample) to reduce standard deviation. A 1-minute integration time was chosen as an optimal trade-off between noise reduction and maintaining sufficient time resolution to track natural variations in CO_2 concentrations accurately. As formula 2, the resampled value Y_i for each minute is calculated as the average of all non-outlier values x_j within that minute.

删除[韩鹏飞]: background noise

$$Y_i = \frac{\sum_{j=1}^{m} x_j}{m} \quad (2)$$

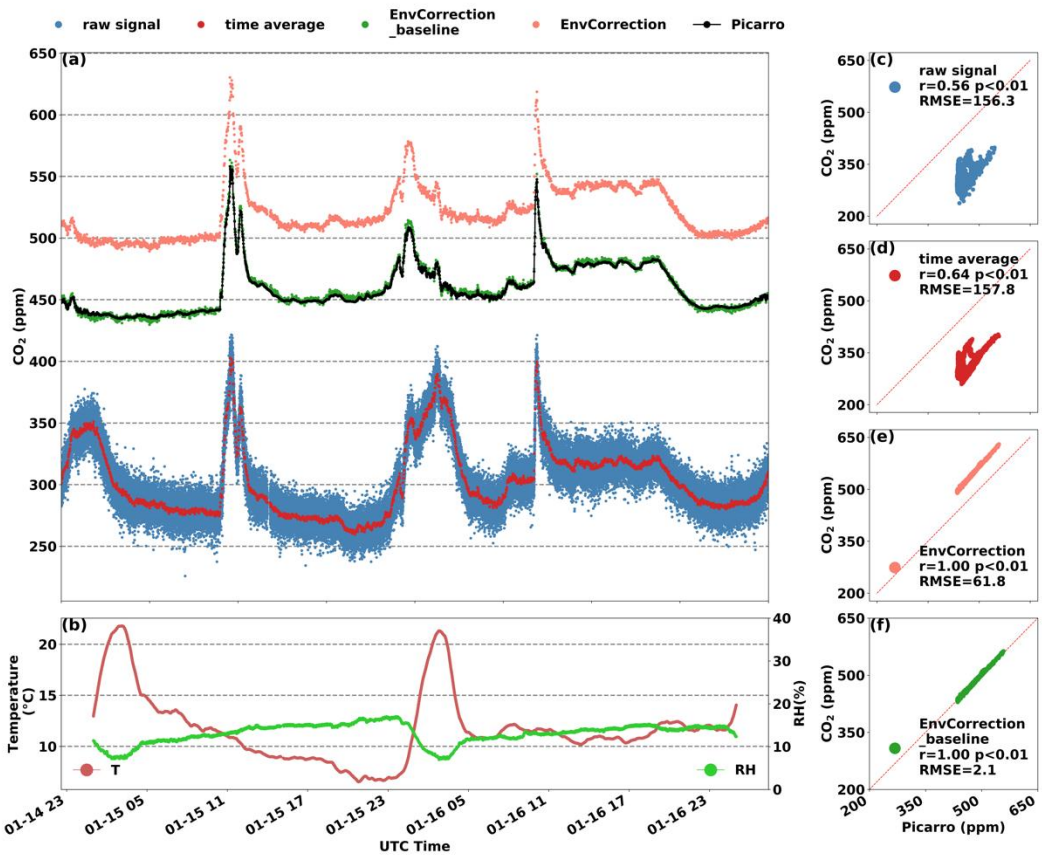

Figure 3. (a) Compared the CO_2 at each processing step, (b) Synchronized monitoring of T and RH. (c-f) The scatterplots of CO_2 measurements form LCS and Picarro instrument at different processing steps, including (c) the raw signal in 2-second resolution, (d) the values after noise reduction at a 1-minute resolution, (e) the CO_2 concentrations after environment corrections and (f) systematic bias correction.

The correction system we developed substantially improves the accuracy of CO_2 measurements through a comprehensive process that includes outlier removal and noise reduction. Fig. 3 shows the main steps of the correction

system, with the data cleaning method described earlier constituting the initial two steps. As shown in Fig.3 (a), the raw signal (blue) undergoes de-specking and denoising (red). However, a noticeable deviation remains between the LCS measurements and the true value, with a correlation coefficient (r-value) of approximately 0.6 (Fig.3(c-d)). The differences mainly come from environmental sensitivity and baseline deviations in concentration.

Similar to the correction standards used in high-precision systems, our LCS units are calibrated using standard gas traceable to the WMO X2007 scale. This calibration adjusts the span and calibrates system bias before deployment. For the typical CO_2 concentration range (400-700ppm), a concentration-dependent offset (ΔC) exists between the time-averaged LCS measurements and the standard gas concentration. Since this concentration dependence varies for each K30 sensor, laboratory corrections are essential for accuracy improvement. Our concentration correction process includes multiple concentration gradients, ensuring applicability to real-world monitoring scenarios. The fitting parameters of ΔC against the measured values are determined through regression analysis, enabling precise correction across the operational range.

$$\Delta C = Y_m - y_0 \quad (3)$$

where, y_0 represents the concentration of standard gas or the high-precision reference instrument (Picarro G2301); Y_m is the minute-averaged values from LCSs.

Environmental calibration was done in an environmental controlled chamber. The environmental sensitivity correction of LCS includes T (10-50 °C with 5 steps), RH (10% -90% with 9 steps), and P compensation correction. This correction is based on sensitivity testing conducted in the laboratory (Martin et al., 2017), with comparisons made against Picarro. Each sensor is assigned unique sensitivity parameters through multivariate regression and iteration analysis.

$$\Delta C = f(a_T, Y_T) + f(a_H, Y_H) + f(\ a_P, Y_P) + f(a_C, Y_C) + \varepsilon \quad (4)$$

where, the baseline correction coefficient is ε; the Y_T, Y_H, Y_P, and Y_C represent the compensation values for the T, RH, P, and concentration sensitivity, respectively, applied to the minute-averaged CO_2 measurement; the a_T, a_H, and a_P are the regression coefficients against T, RH and P respectively, while a_C is the span correction coefficient against concentration.

Thus, the corrected CO_2 can be expressed as:

$$C = Y_m - (f(a_T, Y_T) + f(\ a_P, Y_P) + f(a_H, Y_H) + f(a_C, Y_C) + \varepsilon) \quad (5)$$

The r values between the CO_2 corrected in the final two steps and the Picarro measurements are close to 1 (Fig. 3(e-f)). Additionally, the difference between the environmental correction (pink) and baseline calibration (green) in Fig. 3(a) represents the coefficient ε. After applying these correction steps, the accuracy of the LCS measurements improved to 1-4 ppm compared to Picarro (Liu et al., 2021).

Before deployment, the span and system bias of the LCSs were calibrated. However, once deployed to field stations, LCSs tended to drift on a weekly to monthly scale, necessitating time-dependent drift calibration. We defined S_{cor} as the

starting time of drift and E_{cor} as the time when the drift slope stabilized or when calibration was required, with $\Delta = E_{cor}$-S_{cor}. ΔC_{drift} represents the bias between the concentration C measured by the instrument and the standard concentration C_0 at E_{cor}. Using the formula (6), the drift rate over time (ppm/min) at E_{cor} is calculated as s_t. The b_{cal} is a constant deviation, representing the difference between the baseline and the standard value before long-term drift occurs (at S_{cor}). This value is generally considered zero, since system bias has been calibrated before departure. The error at any time between S_{cor} to E_{cor} can be calibrated to C_{Cor}^{drift} using the following formulas:

$$\Delta C_{drift} = s_t \Delta t + b_{cal} \quad (6)$$

$$C_{Cor}^{drift} = C - \Delta C_{drift} \quad (7)$$

This integrated instrument with environmental correction and drift correction is named as SENSE-IAP.

3. Co-located observation system

Our experiment has been conducted since July 2022 at IAP (Beijing-IAP site, Fig. 4a and 4b). Located in a central urban area with high population density, the Beijing-IAP site is significantly influenced by traffic emissions.

To evaluate the performance of LCS, we developed a synchronous observation system that compares LCS with high-precision instruments. This system includes two SENSE-IAP units (numbered pi688 and pi736), each equipped with three K30 sensors. A cavity ring-down spectrometer (Picarro G2301) was used as the high-precision instrument for CO_2 measurements (Picarro, 2023). The precision and accuracy of the Picarro instrument are better than 0.1 ppm (Yang et al., 2021). At the Beijing-IAP, the Picarro analyzer was calibrated monthly using high-pressure standard gases provided by the Meteorological Observation Center of the China Meteorological Administration (MOC/CMA), which are traceable to the World Meteorological Organization (WMO) X2007 scale.

To ensure long-term synchronous observation between the LCSs and Picarro, deployment enables two sets of instruments measure the same gas mass. This ensures that any differences in observed values only come from the effects of T, RH and P as well as the concentration span, all of which can be adjusted through correction methods. The deployment setup is shown in Fig. 4(b-c).

The instruments were hung on the edge of an open window to directly measure the outdoor air and environmental changes, which are almost the same as field-deployed conditions (Fig. S8), with temperature mainly ranging from 0-40 ℃, and the RH mainly ranging from 0-60%. A partition insulates the LCSs from the indoor space, ensuring the instruments primarily influenced by outdoor environmental conditions. Three K30 sensors and one BME sensor are enclosed in a transparent cover with two 2 mm-diameter ventilation holes at the left-upper and left-lower corners (red circles in Fig.4 c and

设置格式[韩鹏飞]: 字体: （中文）宋体, 10 磅, 字体颜色: 背景 2

删除[其骧 才]: Ambient air is drawn from outside the window using a pump, the intake connected through a pipe equipped with a particulate matter filter and a water dryer. A four-way valve splits the gas stream, directing it to both the LCSs and the Picarro. The instruments were hung on an open window to directly measure the outdoor air and environmental changes, which are the same as field-deployed conditions.

删除[韩鹏飞]: are

删除[韩鹏飞]: rather than indoor air

删除[韩鹏飞]: featuring

d). Air passively diffuses into the pi688 enclosure, while a 4 mm-diameter blue tube connected to the left side of the cover allows an air pump (GAST DOA-P504-BN) to actively draw ambient air from within. Downstream of the pump, the pipe incorporates a capsule 10 μm filter (COBETTER 92WM-LPF1000) to remove particulate matter, and a Nafion drying tube to remove moisture for Picarro use, and moisture is not remove for SENSE-IAP (Fig.4 c). The filtered air is then split by a four-way valve, delivering a 3-5 L/min flow of air to the pi736 and 0.3-0.4 L/min to the Picarro analyzer, and the remained air is vented out at the last outlet.

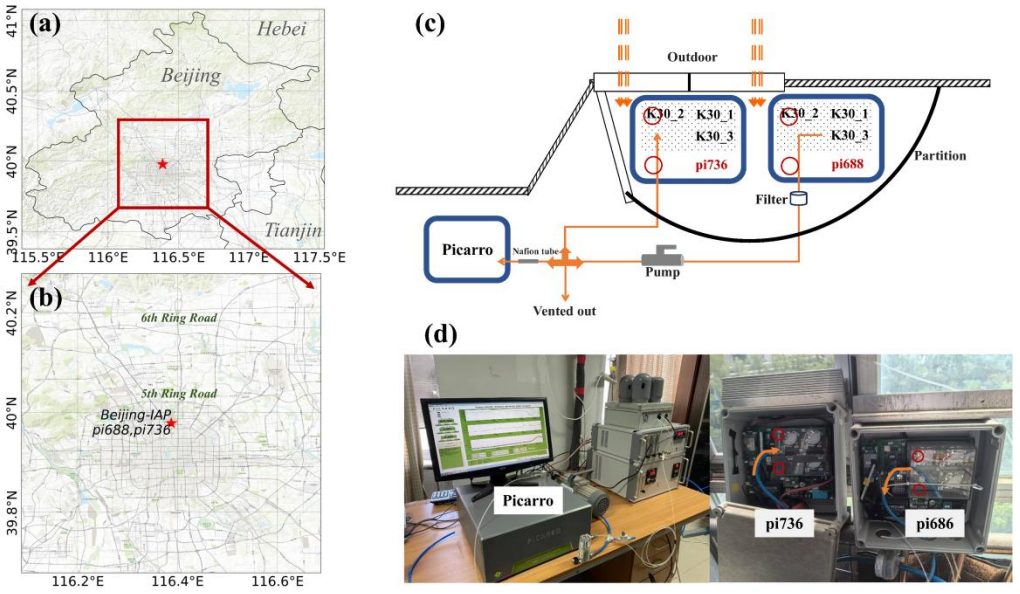

Figure 4. (a) Map of the location of Beijing-IAP in Beijing, (b) Map of the location of Beijing-IAP in the main urban area of Beijing. (c) the diagram of gas flow design for the synchronous observation system, (d) the photographs of the instrument installation setup. The source for the basemap used in subplot (a-b) was from ESRI (https://server.arcgisonline.com/arcgis/rest/services/World_Topo_Map/MapServer).

4. Environmental corrections for field measurements

To separate the influences of short-term environmental factors and long-term drifts, we show the corrections separately. And in order to only focus on the environmental corrections, we removed long-term drifts in this section and discussed this important issue in the following Section 5. Fig. 5 shows the results from environment-corrected SENSE-IAP at the Beijing-IAP site, compared with those from the Picarro system. After approximately two weeks of data collection during both summer and winter, the SENSE-IAP showed highly consistent results with Picarro, with RMSEs of 1.6 ppm in summer and 1.8 ppm in winter. In contrast, the raw CO_2 concentration data from the SenseAir showed a higher RMSE of 6.2 ppm in

设置格式[韩鹏飞]: 字体: （中文）Times New Roman

删除[韩鹏飞]: three

删除[韩鹏飞]: both

设置格式[韩鹏飞]: 突出显示

删除[韩鹏飞]:

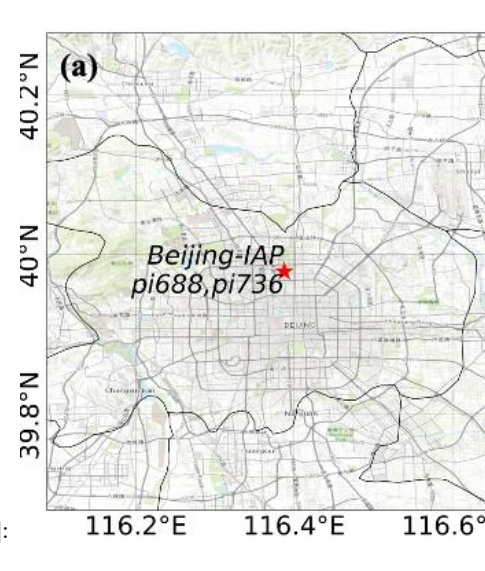

删除[韩鹏飞]: _

summer and 7.0 ppm in winter. Furthermore, the effectiveness of environmental correction is evident across different seasons.

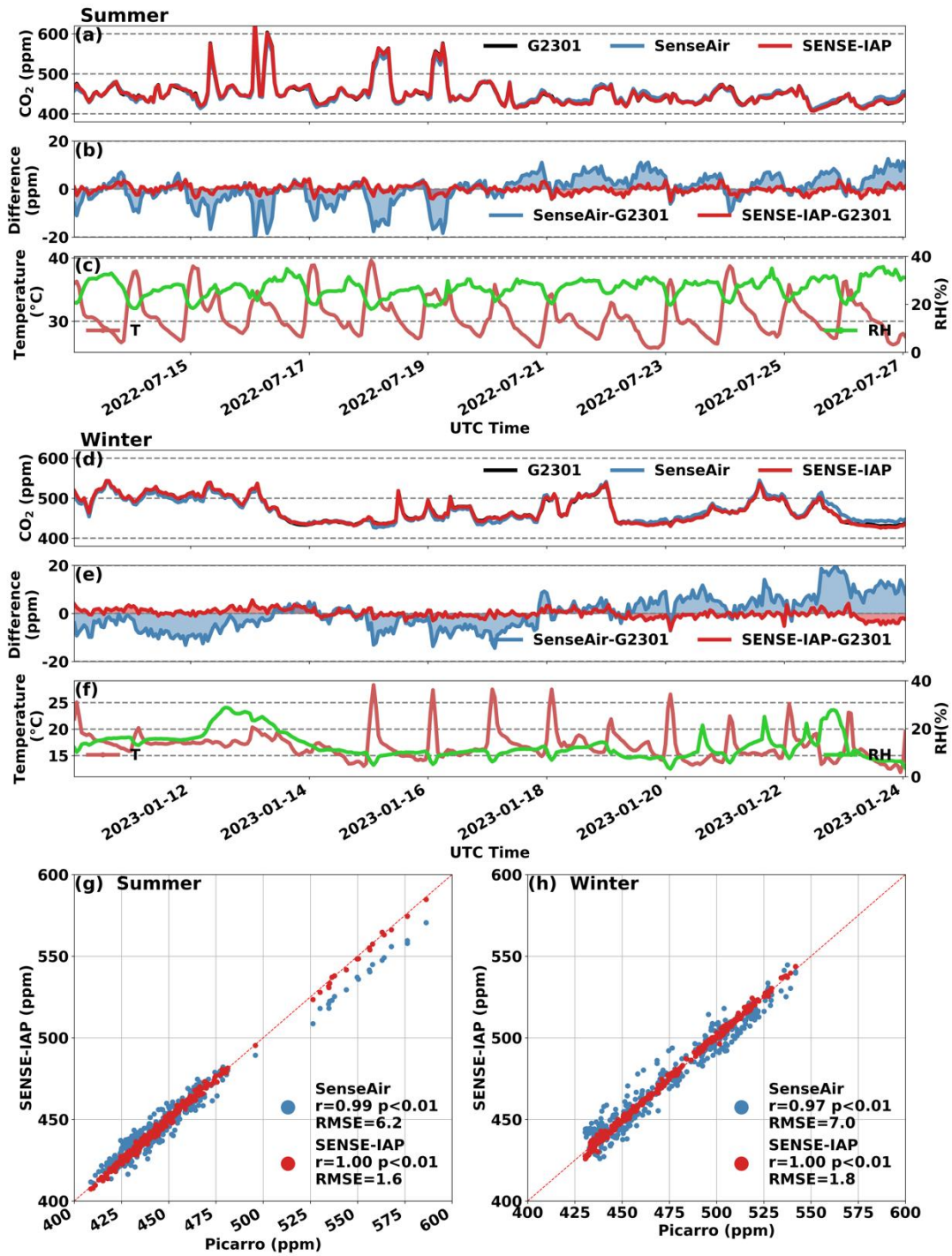

Figure 5: Comparison between hourly CO_2 concentrations measured by the SENSE-IAP and Picarro systems at the Beijing site from July 13th to 27th in 2022 (a-c, g) and January 10th to 24th in 2023 (d-f, h). We compared both the raw CO_2 data from SenseAir (blue) and the environmentally corrected data from SENSE-IAP (red) with that from Picarro (black). The T and RH were measured for the environment inside the instrument.

The correction system effectively adjusted the CO_2 concentration within the 400-700 ppm measurement range. As shown in Fig. 5b, during the period from July 16th to 19th, even when the ambient CO_2 concentration experienced significant fluctuations, the instrument showed high consistency with Picarro. The T and RH detected by the BME sensor were used to monitor the instrument's internal environment. Notably, in winter mornings, sunrise caused a significant temperature increase due to the presence of metal components on the circuit board (Fig. 5f). Our environmental correction successfully corrected for the temperature dependence, as the deviation between the SenseAir and Picarro showed a strongly correlated with temperature in both seasons (Fig. S1a). Additionally, the deviation of SenseAir relative to Picarro was significantly associated with RH in summer (Fig. S1b), and our correction system incorporated humidity, which was related to ambient temperature. Compared to the raw SenseAir data, the consistency of all six sensors improved markedly, with the RMSE decreasing from 5.0 ± 1.0 ppm to 1.3 ± 0.2 ppm in summer and from 6.8 ± 0.8 ppm to 2.0 ± 0.4 ppm in winter (Fig. S2).

删除[其骧 才]: the

Our correction system can perform environmental sensitivity analysis and correction on individual sensors, with the correction efficacy remaining robust across seasonal environmental changes. We further analyzed the daily RMSE of the SENSE-IAP relative to Picarro during 30 months of co-located observation. As shown in Fig. 6a, the daily RMSE of one sensor (pi688-K30) ranged from 1.5 to 4.0 ppm throughout the observation period, with the light blue shadow representing the monthly mean ± standard deviation. The average and median of daily RMSEs for this sensor were less than 2.0 ppm (Fig. 6b), except for an increase to higher than 2 ppm in summer (dark green). Compared to Picarro, the consistency of SENSE-IAP was better in winter, with an RMSE below 2.0 ppm on most days. Except for a few sensors exhibiting slightly higher RMSEs (approximately 3.0 ppm) in spring and autumn (pi732-K30), the daily RMSEs of the six sensors showed no significant seasonal variation (Fig. 6b).

删除[其骧 才]: preform

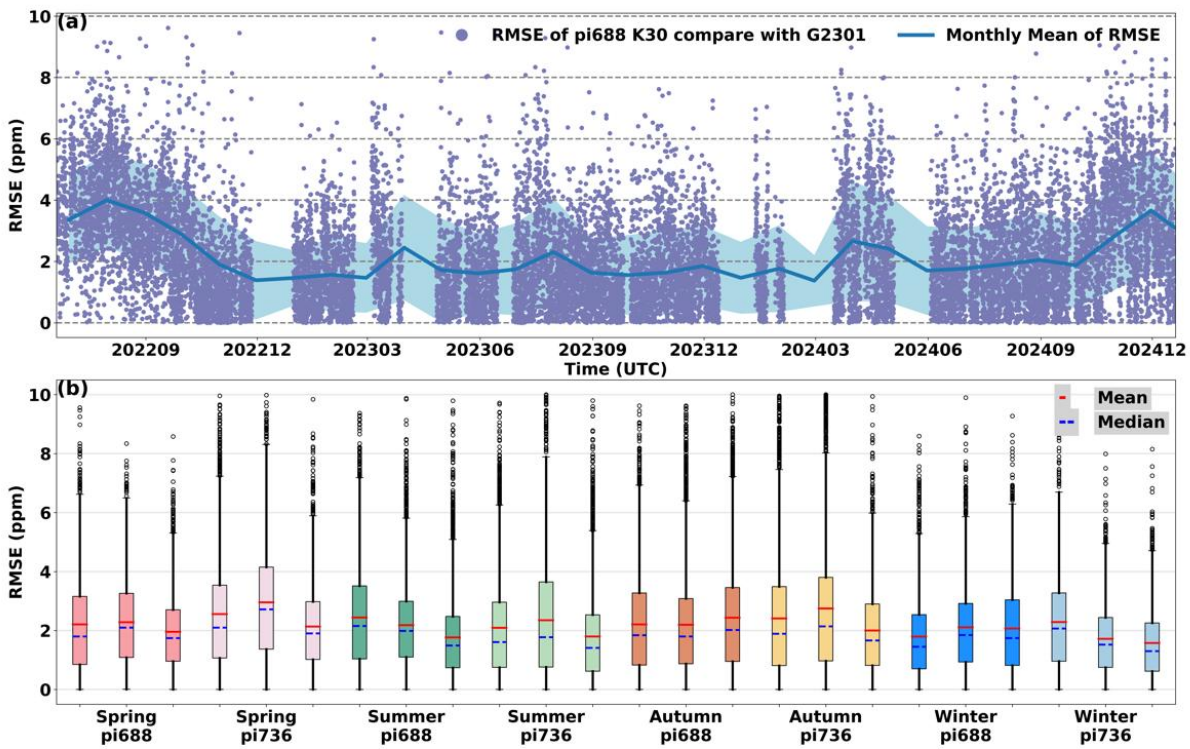

Figure 6. (a) The time series of daily RMSEs for hourly CO_2 concentration relative to Picarro (purple points) from June 2022 to Dec 2024, with a monthly rolling mean (blue line and shadow). (b) Box plot of the daily RMSEs of all six sensors across different seasons. Sensors from the same instrument are represented in the same colors (spring: dark pink/pink; summer: dark green/green; autumn: orange/yellow; and winter: dark blue/blue). Within each box, the red line indicates the mean value, while the blue dashed line represents the median values.

5. Performance of typical long-term drift and correction method

After environmental correction, the six SENSE-IAP sensors were co-located with a Picarro analyzer synchronously for over 30 months. As shown in Fig. 7, two types of long-term drift were identified: 1) a downward drift trend and 2) a seasonal drift cycle. While the environmental correction system effectively corrects the impact of diurnal environmental changes (Fig. 6), significant errors occurred in sensors due to the two types of long-term drift. Without the long-term drift calibration algorithm, the bias of SENSE-IAP could reach 27.9 ppm, with an RMSE of approximately 28.1 ppm (Fig. 7).

During the observation period, all six sensors exhibited long-term downward drifts ranging from 0.1 to 1.2 ppm per month (ppm/mo) (Fig. 7 and Table 2). Among the six sensors deployed in this study, only pi736 K30_3 showed a drift trend of less than 0.1 ppm/mo (Table 2). For sensors such as pi688-K30 and pi688-K30_2, the ΔCO_2 displayed a continuous downward trend over the 30 months, with slopes of 1.2 and 1.0 ppm/mo, respectively (Table 2). Notably, the drift trends for these sensors did not show significantly stabilization over time.

删除[其骧 才]: -
删除[韩鹏飞 [2]]: 1
删除[韩鹏飞 [2]]: 1
删除[韩鹏飞 [2]]: 1

In addition to the downward drift trend, sensors like pi688-K30_3 and pi736-K30 exhibited varying seasonal cycle trends. After six months of deployment, these sensors showed RMSEs of 25.3 and 24.8, respectively (Fig. 7). However, after more than one year of observation, the impact of seasonal drift decreased, and the errors caused by long-term drift were highlighted, resulting in reduced RMSEs as 17.3 and 10 ppm, respectively. And the RMSE evaluation was all done on the same period used to do the drift corrections.

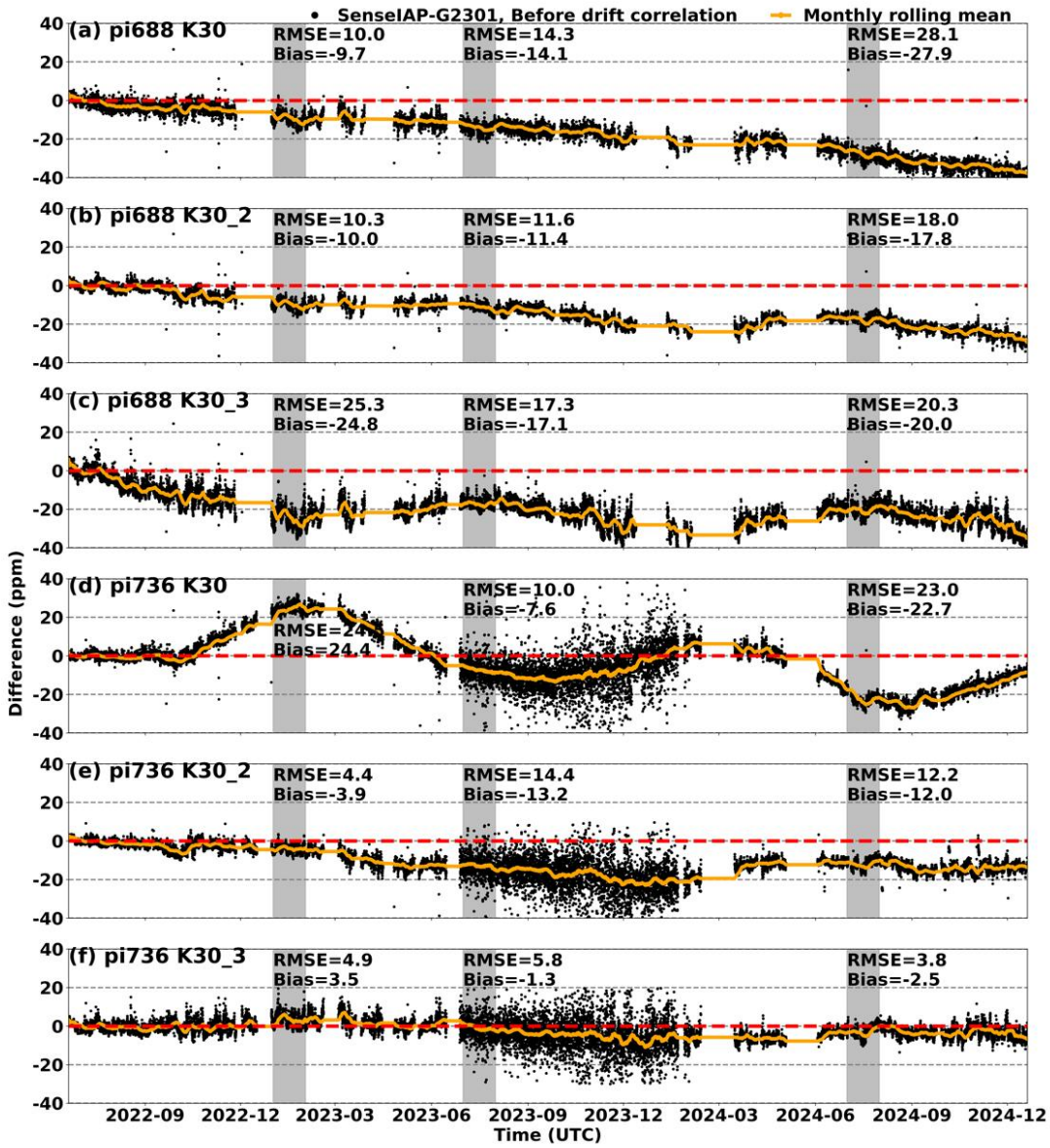

Figure 7: Time series of ΔCO_2 for the six sensors at the Beijing-IAP from June 2022 to Dec 2024 (black), with the monthly rolling mean (yellow line). The gray shadow represents the one-month time range used to evaluate the RMSE and bias for each sensor after half a year, one year, and two years of deployment.

From the perspective of drift magnitude, a significant bias of 5 ppm (approximately 1% of the ambient CO_2 concentration) typically occurred within 3-10 months after calibration, with most cases observed within 5 months. The

seasonal drift cycle occurred on a six-month scale, with maximum errors typically occurring in winter and summer. Therefore, we recommend that the long-term drift calibration frequency of SENSE-IAP should be no less than three months and no longer than six months. In addition, drift calibration should be performed at least once during both winter and summer seasons. If the target monitoring accuracy is within 3 ppm, the drift calibration frequency should be at least every two months, as a 3-ppm bias typically develops within 2-5 months.

Table 2. The Long-term drift trend of six sensors (Unit: ppm/mo)

SENSE-IAP	**pi688**			**pi736**		
Slope (ppm/mo)	s1	s2	s3	s1	s2	s3
drift in the first year	-1.2	-1.0	-1.4	-0.6	-1.1	-0.1
drift in the second year	-1.2	-0.5	-0.2	-1.3	0.1	-0.1

The method for the long-term drift calibration is as follows. According to functions 6-7, we illustrate our long-term drift calibration method by focusing on the first year of observation. At the start of the observation period (Jun 2022), we adjusted the baseline of the six sensors. We designated the initial calibration time point as S_{cor} for the first observation period (Jun 2022 to Jan 2023). The inflection point of the drift trend in Feb 2023 was identified as E_{cor} for the first period and as S_{cor} for the second period of the observation (Jan 2023 to Sep 2023). The E_{cor} for the second period was set to Sep 2023 in this study. We applied the linear calibration method between these two time points for both periods of the drift trend. After calibration, the CO_2 concentrations from the six sensors showed strong consistency with the Picarro, with an RMSE ranging from 2.4-3.0 ppm (Fig. 8).

删除[韩鹏飞 [2]]: 1

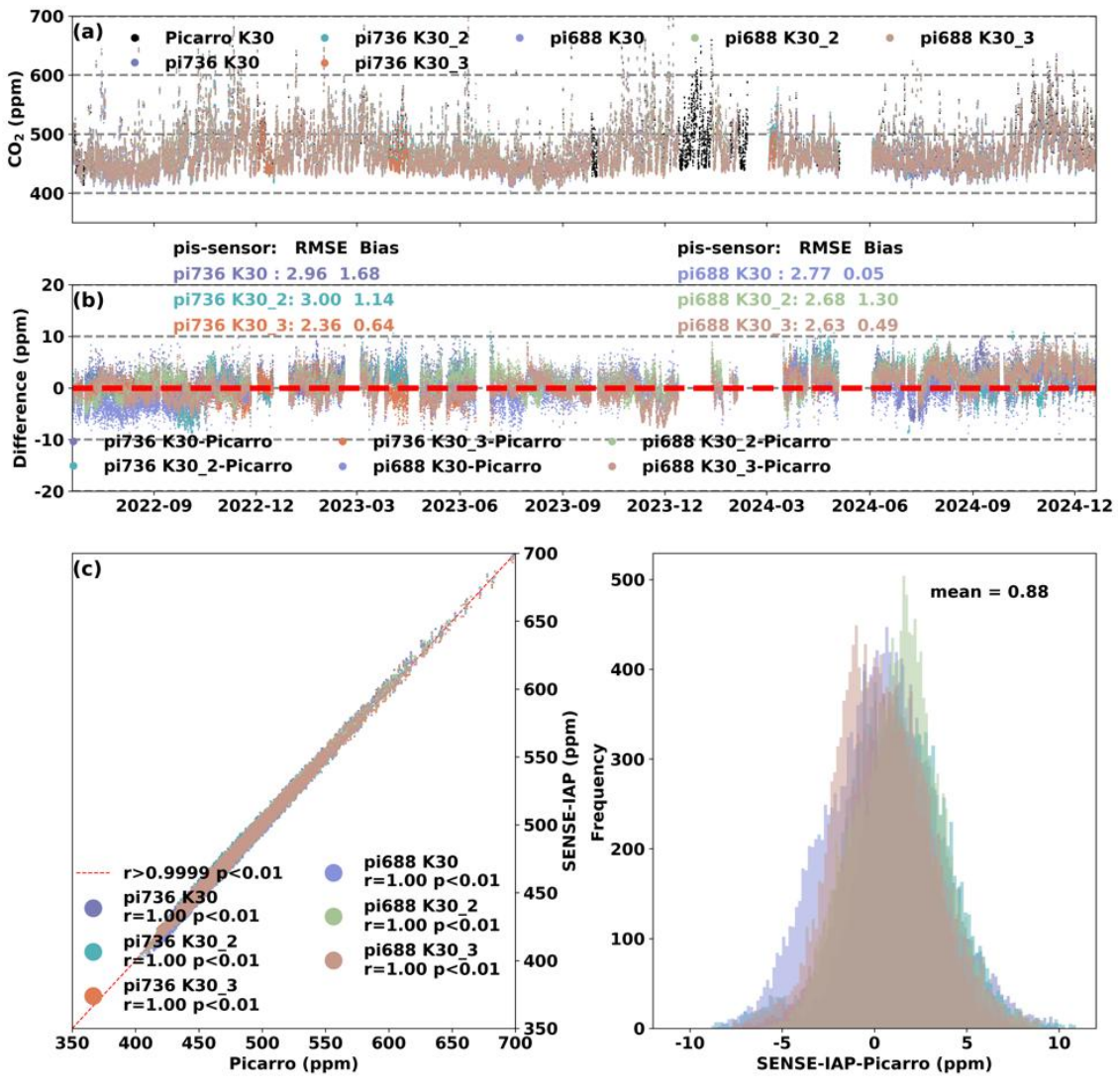

Figure 8: (a) Comparison of hourly CO_2 concentrations measured by six sensors and Picarro at Beijing- IAP from June 2022 to Dec 2024; (b) the time series of ΔCO_2; (c) scatter plot of SENSE-IAP and Picarro; (d) histogram plot of the ΔCO_2.

It should be noted that due to the loose connection of ventilation pipeline between Jul 2023 to Mar 2024, the CO_2 concentration measured by pi736 and Picarro were not strictly synchronized. This issue led to a relatively lower short-term monitoring accuracy during this period, primarily due to the lag effect caused by air diffusion. To assess the actual hourly monitoring accuracy of SENSE-IAP, we excluded data from this period. Without this exclusion, the RMSE for pi736 would have been 3.9-4.5 ppm (Fig. S3). However, to ensure the completeness and robustness of the long-term drift analysis, we retained samples from this period, allowing for a more comprehensive evaluation of drift trends over time.

6. Comparison of data quality across multiple levels over a long-term scale

As previously mentioned, the correction system effectively corrected the sensors' short-term environmental dependence. By applying a linear calibration method at least every three months, we can calibrate the time-dependent drift of LCSs and

resolve residual seasonal cycles that the environmental correction system cannot fully resolve. This seasonal variation is prominently reflected in the original electrical signal (raw signal). As shown in Figure S4(b), we eliminated the influence of short-term environment changes through a 24-hour running mean, revealing that the seasonal drift cycle in the raw signal can reach up to 100ppm, with an RMSE of 38.2 and a bias of -21.1 ppm (Table 3).

The defining characteristic of medium-precision low-cost sensors is the presence of long-term drift. This drift, which exhibits a downward trend, is observed in all sensors, with variations only in the drift rate (Fig.S5). Long-term drifts resulted in an RMSE of 15.8 and a bias of -12.0 for the LCS, respectively (Table 3). Although seasonal cycle does not significantly alter the overall trend of long-term drift, seasonal environmental variations can introduce errors of up to 25 ppm if baseline calibration are performed only annually (Fig. 7). Therefore, we recommend that baseline calibration be conducted at least every six months, ideally during both winter and summer.

The data provided by the SenseAir manufacturer were corrected for temperature sensitivity using the default temperature parameters. The long-term drift was calibrated using a so-called ABS algorithm, which employs periodic one-point calibration in SenseAir, assuming that the minimum value of CO_2 concentration is 400 ppm in fresh air (SenseAir-Corrected data). However, due to the constant assumption of fresh air concentration, coupled with the carbon absorption of vegetation in summer and the higher emissions in winter, the SenseAir-Corrected data exhibit a fluctuating trend of approximately 20 ppm, with higher values in summer and lower values in winter. Consequently, the bias of SenseAir-Corrected data can be -3.3 ± 1.4 ppm, with an RMSE of 12.1 ± 2.0 ppm (Fig. S6, Table 3). In contrast, the drift-calibrated SENSE-IAP data demonstrate a much smaller bias (0.8 ± 0.4 ppm) and an 80% improvement in accuracy, with an RMSE of 2.4 ± 0.2 ppm (Fig.S7, Table 3).

删除[韩鹏飞 [2]]: 2

删除[韩鹏飞 [2]]: 2

删除[其骧 才]: manufacture

删除[其骧 才]: were

删除[韩鹏飞 [2]]: 2

删除[韩鹏飞 [2]]: 2

Table 3: Evaluation parameters of the CO_2 concentration measured by K30 sensors compared to those from Picarro, including SenseAir-Corrected values, Raw signal, and SENSE-IAP at the Beijing-IAP from June 2022 to December 2024 (unit: ppm).

Data Type	**SenseAir-Corrected**		**Raw signal**		**SENSE-IAP-Env-Corrected**		**SENSE-IAP-Env+Drift-Corrected**	
Sensors	RMSE	Bias	RMSE	Bias	RMSE	Bias	RMSE	Bias
Pi688 K30	15.9	-5.7	34.4	-20.2	20.1	-16.9	2.2	0.1
Pi688 K30_2	10.1	-3.1	35.1	-19.0	15.7	-13.6	2.4	1.3
Pi688 K30_3	10.2	-3.3	45.2	-24.2	21.5	-20.0	2.3	0.5
Pi736 K30	10.8	-1.1	22.0	-11.8	13.5	-3.5	2.6	1.1
Pi736 K30_2	13.0	-2.6	38.4	-23.0	14.3	-10.8	2.8	1.0
Pi736 K30_3	12.5	-4.2	53.9	-28.1	9.8	-7.0	2.2	0.7
Mean	12.1	-3.3	38.2	-21.1	15.8	-12.0	2.4	0.8
SD	2.0	1.4	9.9	-5.1	4.0	5.6	0.2	0.4

*According to the statistical results of 24-hour running means.

7. Seasonal drift cycle effects on SENSE-IAP

As shown in Fig. S8, the seasonal variations observed before instrument linear calibration were correlated with T, RH and P. The ΔCO_2 between pi736-K30 and Picarro significantly correlated with all three environmental factors, with r values of -0.58, -0.46, and 0.33 against T, RH and P, respectively. In contrast, the relationship between pi688-K30_3 and environmental factors was opposite to that of pi736-K30, with r values of 0.33, 0.5, and -0.6 against T, RH and P, respectively. Considering seasonal phase differences between CO_2 concentration changes and environmental factors, this seasonal deviation was likely attributable not only to insufficient environmental compensation but also to the influence of seasonal effects on the instrument's physical properties. For instance, changes in the sensor's optical cavity size caused by thermal expansion and cold contraction can change the optical path-lengths, subsequently affecting the pressure within the optical cavity and the strength of infrared CO_2 absorption (Yao et al., 2023). However, this hypothesis cannot fully explain why the two sensors, pi688 K30_3 and pi736 K30, exhibited opposite drift directions during the same season.

Long-term drift is typically observed in low- and mid-cost NDIR CO_2 sensors. While our findings provide valuable references for K30 sensors, the recommended calibration frequency and observed seasonal cycle characteristics may be also applicable to other similar NDIR sensors, and the calibration method we used is universal and helpful in long-term drift corrections. For other NDIR sensors, we recommend selecting several samples to conduct co-location with high-precision instrument under field conditions for at least one year to study their full characteristics. This extended co-location period is

删除[韩鹏飞 [2]]: **2**

删除[韩鹏飞]: not

删除[韩鹏飞]: directly

删除[韩鹏飞]: This is because both the slope of long-term drift and its seasonal drift cycle may depend on the supporting hardware and deployment environments.

删除[韩鹏飞]: undergo

删除[韩鹏飞]: s/standard gases

删除[韩鹏飞]: quasi-

essential to comprehensively characterize both long-term drifts and the seasonal drift cycle. The results will provide critical guidance for remote calibration of high-density networks using this type of sensor. Furthermore, another practical substitute method is using standard gas, and the calibration frequency from the experience of this study is recommended at least one-three month.

删除[韩鹏飞]: trend

8. Conclusions

We evaluated low-cost NDIR CO_2 sensors using Picarro as a reference instrument. Our environmental correction system effectively corrected the impact of short-term daily environmental changes by assigning unique environmental sensitivity parameters to each sensor. This approach reduces the short-term RMSE from 5.9 ± 1.2 ppm for SenseAir to 1.6 ± 0.5 ppm for SENSE-IAP. The correction system demonstrates robustness against seasonal environmental variations, maintaining a daily RMSE of 1-3 ppm.

Based on a 30-month observation, we recommend that the calibration frequency for long-term drifts not exceed six months. For optimal performance and to ensure the target monitoring accuracy remains within 1% of the ambient CO_2 concentration, a three-month calibration interval is recommended. If standard instruments, standard gases (which are generally easier to obtain), or other reliable concentration references such as model simulations are available, long-term drift can be linearly corrected at the seasonal scale.

Consequently, after deployment, even with significant environmental changes around the instrument, there is no need to frequently bring the instruments back to the laboratory for re-correction of environmental impacts. After the long-term drift calibration, the RMSE of SENSE-IAP remains 2.4 ± 0.2 ppm even after 30 months of operation. This performance enables long-term deployment of the instruments, significantly reducing the maintenance costs associated with LCS.

Supporting information

The supplementary information is available online.

Data availability statement

The data used to generate the figures in this manuscript are available at https://doi.org/10.6084/m9.figshare.29310890.v3

删除[韩鹏飞]: 2

删除[韩鹏飞]: Raw data can be given upon reasonable request to the corresponding authors.

Competing interests

The authors declare that they have no conflicts of interest.

Funding

This research was supported by the National Key R&D Program of China (No. 2023YFC3705500 and 2017YFB0504000); Jinan Carbon Monitoring and Evaluation Pilot Project (grant no. SDGP370100000202202001740); the Qiluzhongke Institute

of Carbon Neutrality Program of Jinan Dual Carbon Simulator; and the CAS Proof of Concept Program: Carbon Neutrality-oriented Urban Carbon Monitoring System and Its Industrialization (grant no. CAS-GNYZ-2022).

Author contributions

NZ, PFH and QXC conceived and designed the study. QXC and PFH collected and analyzed the datasets. XYY, CX, and ZJW discussed the sensor results. QXC led the writing of the paper with contributions from all the coauthors. All coauthors contributed to the descriptions and discussions of the manuscript.

Acknowledgments

We thank Mr. Cory Martin, Mr. Di Liu, Mr. Yinan Wang, Mr. Ming Cui, Mr. Jin Guo, Mr. Zhimin Zhang, and Mr. Yang Zi for their help in the SENSE-IAP instrument development, calibration and deployments.

References

SenseAir: LP8 Product Sheet: https://rmtplusstoragesenseair.blob.core.windows.net/docs/Dev/publicerat/PSH1233.pdf, last access: 6 March 2019.

SenseAir: K30 products sheets: https://rmtplusstoragesenseair.blob.core.windows.net/docs/publicerat/PSP110.pdf, last access: 6 March 2022.

Asimow, N. G., Turner, A. J., and Cohen, R. C.: Sustained Reductions of Bay Area CO2 Emissions 2018–2022, Environ. Sci. Technol., 58, 6586–6594, https://doi.org/10.1021/acs.est.3c09642, 2024.

Bao, Z., Han, P., Zeng, N., Liu, D., Cai, Q., Wang, Y., Tang, G., Zheng, K., and Yao, B.: Observation and modeling of vertical carbon dioxide distribution in a heavily polluted suburban environment, Atmospheric Ocean. Sci. Lett., 13, 371–379, https://doi.org/10.1080/16742834.2020.1746627, 2020.

Bigi, A., Mueller, M., Grange, S. K., Ghermandi, G., and Hueglin, C.: Performance of NO, NO_2 low cost sensors and three calibration approaches within a real world application, Atmospheric Meas. Tech., 11, 3717–3735, https://doi.org/10.5194/amt-11-3717-2018, 2018.

Cai, Q., Han, P., Pan, G., Xu, C., Yang, X., Xu, H., Ruan, D., and Zeng, N.: Evaluation of Low-Cost CO2 Sensors Using Reference Instruments and Standard Gases for Indoor Use, Sensors, 24, https://doi.org/10.3390/s24092680, 2024.

Cai, Q., Wang, Z., Han, P., Zeng, N., Nie, X., Yang, X., Wang, Z., and Gao, S.: The Enhancement and Variation in the Carbon Dioxide Concentration in a Typical Industrial Park in the Northern China, Aerosol Sci. Eng., https://doi.org/10.1007/s41810-025-00286-4, 2025.

Delaria, E. R., Kim, J., Fitzmaurice, H. L., Newman, C., Wooldridge, P. J., Worthington, K., and Cohen, R. C.: The Berkeley Environmental Air-quality and CO_2 Network: field calibrations of sensor temperature dependence and assessment of network scale CO_2 accuracy, Atmospheric Meas. Tech., 14, 5487–5500, https://doi.org/10.5194/amt-14-5487-2021, 2021.

Grange, S. K., Rubli, P., Fischer, A., Brunner, D., Hueglin, C., and Emmenegger, L.: The ZiCOS-M CO_2 sensor network: measurement performance and CO_2 variability across Zurich, Atmospheric Chem. Phys., 25, 2781–2806, https://doi.org/10.5194/acp-25-2781-2025, 2025.

Grimmond, C. S. B., King, T. S., Cropley, F. D., Nowak, D. J., and Souch, C.: Local-scale fluxes of carbon dioxide in urban environments: methodological challenges and results from Chicago, Environ. Pollut., 116, S243–S254, https://doi.org/10.1016/S0269-7491(01)00256-1, 2002.

Gurney, K. R., Razlivanov, I., Song, Y., Zhou, Y., Benes, B., and Abdul-Massih, M.: Quantification of Fossil Fuel CO2 Emissions on the Building/Street Scale for a Large U.S. City, Environ. Sci. Technol., 46, 12194–12202, https://doi.org/10.1021/es3011282, 2012.
Hagan, D. H., Isaacman-VanWertz, G., Franklin, J. P., Wallace, L. M. M., Kocar, B. D., Heald, C. L., and Kroll, J. H.: Calibration and assessment of electrochemical air quality sensors by co-location with regulatory-grade instruments, Atmospheric Meas. Tech., 11, 315–328, https://doi.org/10.5194/amt-11-315-2018, 2018.
Han, P., Yao, B., Cai, Q., Chen, H., Sun, W., Liang, M., Zhang, X., Zhao, M., Martin, C., Liu, Z., Ye, H., Wang, P., Li, Y., and Zeng, N.: Support Carbon Neutral Goal with a High-Resolution Carbon Monitoring System in Beijing, Bull. Am. Meteorol. Soc., 105, E2461–E2481, https://doi.org/10.1175/BAMS-D-23-0025.1, 2024.
Han, P., Felix, V., Dominik, B., Tyler, B., Qixiang, C., Zhiqiang, L., Ning, Z., and Olivier, L.: Chapter 18: Dense Networks Of Mid-Low Cost CO2 Sensors, in IG3IS Urban Greenhouse Gas Emission Observation and Monitoring Good Research Practice Guidelines, WMO GAW Report 2025, available at https://www.dropbox.com/scl/fi/vuk8ad8bdui8ibekefuob/IG3ISUrbanGuidelines_FinalDraft_May2025.docx?rlkey=zmu8nwaj6dgenssuxct9jihqv&st=t7wtafz0&dl=0, accessed on June 16th 2025., 2025.
He, J., Li, Z., Zhang, X., Wang, H., Dong, W., Chang, S., Ou, X., Guo, S., Tian, Z., Gu, A., Teng, F., Yang, X., Chen, S., Yao, M., Yuan, Z., Zhou, L., and Zhao, X.: Comprehensive report on China's Long-Term Low-Carbon Development Strategies and Pathways, Chin. J. Popul. Resour. Environ., 18, 263–295, https://doi.org/10.1016/j.cjpre.2021.04.004, 2020.
Huang, Y., Liu, G., Bo, Y., Wang, J., Cao, M., Lu, X., and He, K.: Beijing–Tianjin–Hebei Coordinated Development toward the Carbon Peaking and Carbon Neutrality Goals. , Strateg. Study CAE, 25, 160–172, 2023.
Kellett, R., Christen, A., Coops, N. C., van der Laan, M., Crawford, B., Tooke, T. R., and Olchovski, I.: A systems approach to carbon cycling and emissions modeling at an urban neighborhood scale, Landsc. Urban Plan., 110, 48–58, https://doi.org/10.1016/j.landurbplan.2012.10.002, 2013.
Lateb, M., Meroney, R. N., Yataghene, M., Fellouah, H., Saleh, F., and Boufadel, M. C.: On the use of numerical modelling for near-field pollutant dispersion in urban environments–A review., Environ. Pollut., 208 Pt A, 271–283, 2016.
Lian, J., Laurent, O., Chariot, M., Lienhardt, L., Ramonet, M., Utard, H., Lauvaux, T., Bréon, F.-M., Broquet, G., Cucchi, K., Millair, L., and Ciais, P.: Development and deployment of a mid-cost CO_2 sensor monitoring network to support atmospheric inverse modeling for quantifying urban CO_2 emissions in Paris, Atmospheric Meas. Tech., 17, 5821–5839, https://doi.org/10.5194/amt-17-5821-2024, 2024.
Liu, D., Sun, W., Zeng, N., Han, P., Yao, B., Liu, Z., Wang, P., Zheng, K., Mei, H., and Cai, Q.: Observed decreases in on-road CO_2 concentrations in Beijing during COVID-19 restrictions, Atmospheric Chem. Phys., 21, 4599–4614, https://doi.org/10.5194/acp-21-4599-2021, 2021.
Lopez-Coto, I., Ghosh, S., Prasad, K. R., and Whetstone, J.: Tower-based greenhouse gas measurement network design—The National Institute of Standards and Technology North East Corridor Testbed, Adv. Atmospheric Sci., 34, 1095–1105, 2017.
Martin, C. R., Zeng, N., Karion, A., Dickerson, R. R., Ren, X., Turpie, B. N., and Weber, K. J.: Evaluation and environmental correction of ambient CO_2 measurements from a low-cost NDIR sensor, Atmospheric Meas. Tech., 10, 2383–2395, https://doi.org/10.5194/amt-10-2383-2017, 2017.
Miles, N. L., Davis, K. J., Richardson, S. J., Lauvaux, T., Martins, D. K., Deng, A. J., Balashov, N., Gurney, K. R., Liang, J., Roest, G., Wang, J. A., and Turnbull, J. C.: The influence of near-field fluxes

on seasonal carbon dioxide enhancements: results from the Indianapolis Flux Experiment (INFLUX), Carbon Balance Manag., 16, 4, https://doi.org/10.1186/s13021-020-00166-z, 2021.
Müller, M., Graf, P., Meyer, J., Pentina, A., Brunner, D., Perez-Cruz, F., Hüglin, C., and Emmenegger, L.: Integration and calibration of non-dispersive infrared (NDIR) CO2 low-cost sensors and their operation in a sensor network covering Switzerland, Atmospheric Meas. Tech., 13, 3815–3834, https://doi.org/10.5194/amt-13-3815-2020, 2020.
Picarro: G2301 Analyzer Datasheet: https://www.picarro.com/sites/default/files/product_documents/Picarro_G2301%20Datasheet_230306.pdf (last access: 20 May 2025), 2023.
Shusterman, A. A., Teige, V. E., Turner, A. J., Newman, C., Kim, J., and Cohen, R. C.: The BErkeley Atmospheric CO_2 Observation Network: initial evaluation, Atmospheric Chem. Phys., 16, 13449–13463, https://doi.org/10.5194/acp-16-13449-2016, 2016.
Shusterman, A. A., Kim, J., Lieschke, K. J., Newman, C., Wooldridge, P. J., and Cohen, R. C.: Observing local CO2 sources using low-cost, near-surface urban monitors, Atmospheric Chem. Phys., 18, 13773–13785, https://doi.org/10.5194/acp-18-13773-2018, 2018.
Turner, A. J., Shusterman, A. A., McDonald, B. C., Teige, V., Harley, R. A., and Cohen, R. C.: Network design for quantifying urban CO_2 emissions: assessing trade-offs between precision and network density, Atmospheric Chem. Phys., 16, 13465–13475, https://doi.org/10.5194/acp-16-13465-2016, 2016.
Vaisala: GMP343 Carbon Dioxide Probe Datasheet, https://docs.vaisala.com/v/u/B210688EN-H/en-US, last access: 6 March 2020.
Wada, R., Pearce, J. K., Nakayama, T., Matsumi, Y., Hiyama, T., Inoue, G., and Shibata, T.: Observation of carbon and oxygen isotopic compositions of CO2 at an urban site in Nagoya using Mid-IR laser absorption spectroscopy, Atmos. Environ., 45, 1168–1174, https://doi.org/10.1016/j.atmosenv.2010.10.015, 2011.
Wu, L., Broquet, G., Ciais, P., Bellassen, V., Vogel, F., Chevallier, F., Xueref-Remy, I., and Wang, Y.: What would dense atmospheric observation networks bring to the quantification of city CO_2 emissions?, Atmospheric Chem. Phys., 16, 7743–7771, https://doi.org/10.5194/acp-16-7743-2016, 2016.
Yang, Y., Zhou, M., Wang, T., Yao, B., Han, P., Ji, D., Zhou, W., Sun, Y., Wang, G., and Wang, P.: Spatial and temporal variations of CO2 mole fractions observed at Beijing, Xianghe, and Xinglong in North China, Atmospheric Chem. Phys., 21, 11741–11757, https://doi.org/10.5194/acp-21-11741-2021, 2021.
Yao, G., Li, Y., Shang, Q., and Fan, H.: Research on Temperature Compensation of Optical Fiber MEMS Pressure Sensor Based on Conversion Method, Photonics, 10, https://doi.org/10.3390/photonics10010022, 2023.
Zeng, N., Han, P., Liu, Z., Liu, D., Oda, T., Martin, C. R., Liu, Z., Yao, B., Sun, W., Wang, P. C., Cai, Q., Dickerson, R., and Maksyutov, S.: Global to local impacts on atmospheric CO2 from the COVID-19 lockdown, biosphere and weather variabilities, Environ. Res. Lett., 17, 2021.
Zeng, N., Jiang, K., Han, P., Hausfather, Z., Cao, J., Kirk-Davidoff, D., Ali, S., and Zhou, S.: The Chinese Carbon-Neutral Goal: Challenges and Prospects, Adv. Atmospheric Sci., 39, 1229–1238, 2022.